Original Article

Asian Pacific Journal of Tropical Biomedicine

journal homepage: www.apjtb.org

doi: 10.4103/2221-1691.326097

Impact Factor: 1.55

Effects of Sirt1 on proliferation, migration, and apoptosis of endothelial progenitor cells in peripheral blood of SD rats with chronic obstructive pulmonary disease

Dong-Mei Sun[1,4#], Jin-Jian Yao[2#], Zhan-Ling Dong[3#], Jin Qian[1], Qi-Feng Huang[1], Yuan-Tian Sun[3✉], Xiao-Ran Liu[1✉]

[1]*The First Affiliated Hospital of Hainan Medical University, Haikou, China*

[2]*Emergency Center of Hainan General Hospital Affiliated to Hainan Medical University, Haikou, China*

[3]*Hainan Medical University, Haikou, China*

[4]*Shandong Heze Mudan People's Hospital, Heze, China*

ABSTRACT

Objective: To explore the effect of Sirt1 on the function of endothelial progenitor cells (EPCs) in rats with chronic obstructive pulmonary disease (COPD).

Methods: A rat COPD model was established *via* smoking and endotoxin administration for three months. The peripheral circulating EPCs were isolated by gradient centrifugation, and their functions, cell cycle distribution, apoptosis, and Sirt1 expression were examined. The function changes of EPCs in the presence or absence of Sirt1 agonist and inhibitor were estimated; meanwhile, the expressions of Sirt1, FOXO3a, NF-κB, and p53 were also evaluated.

Results: The proliferation, adhesion, and migration of EPCs decreased while the apoptosis rate was increased in the COPD rats. The expression of Sirt1 protein in EPCs of the COPD group was significantly lower than that in the control group (P<0.01). The overexpression of the *Sirt1* gene using a gene transfection technique or Sirt1 agonists (SRT1720) improved the proliferation, migration, and adhesion, and decreased the apoptosis of EPC. However, Sirt1 inhibitor (EX527) decreased EPC functions in the COPD group. The effect of Sirt1 expression on EPC function may be related to reduction of FOXO3a and increase of NF-κB and p53 activity.

Conclusions: Increased expression of Sirt1 can improve the proliferation and migration of EPCs and reduce their apoptosis in COPD rats. This change may be related to FOXO3a, NF-κB, and p53 signaling pathways.

KEYWORDS: Chronic obstructive pulmonary disease; Endothelial progenitor cells; Sirt1; Proliferation; Migration; Adhesion; Apoptosis; FOXO3a; NF-κB; p53; Rat

1. Introduction

Chronic obstructive pulmonary disease (COPD) is prevalent throughout the world. In 2017, the incidence of COPD worldwide was approximately 299.4 million and 3.2 million people died from the disease[1,2]. A Chinese epidemiological survey found that the prevalence of COPD in people over 40 years old was 13.6% in 2014-2015[3]. The number of deaths due to COPD worldwide ranked fourth after cardiovascular disease, tumors, and cerebrovascular disease. In 2015, COPD has become the third leading cause of death throughout the world, just following ischaemic heart disease and cerebrovascular disease; additionally, a third of COPD deaths are attributed to cardiovascular diseases[4]. COPD is an important

✉To whom correspondence may be addressed. E-mail: 297008591@qq.com (Yuan-Tian Sun), liuxiaoran3192@163.com (Xiao-Ran Liu)
#These authors contributed equally to this work.

How to cite this article: Sun DM, Yao JJ, Dong ZL, Qian J, Huang QF, Sun YT, et al. Effects of Sirt1 on proliferation, migration, and apoptosis of endothelial progenitor cells in peripheral blood of SD rats with chronic obstructive pulmonary disease. Asian Pac J Trop Biomed 2021; 11(10): 429-439.

Article history: Received 28 April 2021; Revision 29 May 2021; Accepted 27 August 2021; Available online 30 September 2021

(though frequently under-recognised) risk factor for cardiovascular diseases[5] such as angina, myocar-dial infarction, heart failure, sudden cardiac arrest, atrial fibrillation[6].

It has been reported that endothelial function is impaired in the early stages of COPD, and the processes of injury and repair were imbalanced due to endothelial dysfunction[7]. Endothelial progenitor cells (EPCs) promote the dynamic balance of blood vessels. Many studies have shown that circulating EPCs are decreased and dysfunctional in patients with COPD[8-11]. Cell number reduction and dysfunction of EPCs are affected by many factors, but it is unclear whether EPC function in the COPD model is related to intracellular Sirt1. Sirt1 is a member of the Sirtuin family and has a conserved catalytic and a nicotinamide adenine dinucleotide linker domain[12]. Sirt1 is widely expressed in mammals, primarily in cell nuclei. It is a nuclear protein that exerts its anti-oxidative stress, anti-inflammatory, and anti-cell aging effects by deacetylating target proteins[13]. Sirt1 regulates oxidative stress but is also regulated by oxidative stress. Metabolic response, aging, chronic disease, and various extracellular stimuli can affect Sirt1 protein levels in the processes of metabolism, senescence, and chronic disease and in response to various external stimuli. It has been demonstrated that the levels of Sirt1 are reduced in lung epithelial cells, endothelial cells, and macrophages in smoking and COPD patients[14,15]. Whether the expression of Sirt1 is decreased in EPCs cells remains unclear. This study aims to explore whether the function and number of EPCs in COPD rats is related to Sirt1.

2. Materials and methods

2.1. Reagents and drugs

EBM-2 culture medium (Lonza, USA), ficoll hypaque 1.077 (Haoyang, Tianjin, China), lipopolysaccharide (Solarbio, Beijing, China), CCK-8 kit (Dojindo Laboratories, Japan), FITC-coupled annexin-V apoptosis detection kit (BD Biosciences, USA), cell cycle and apoptosis kit (Beyotime Biotechnology, Shanghai, China), FITC-UEA-I/ DiI-acLDL (Proteintech, USA), PCDH-CMV-EF1-copGFP-Sirt1 (LabGene, Guangzhou, China), SRT1720/EX527 (Sigma-Aldrich, USA), reverse transcription kit (Thermo Fisher, USA), rabbit monoclonal antibodies to Sirt1/β-actin (ab189494/ ab115777, Abcam, UK), rabbit monoclonal antibodies to p53/NF-κB/FOXO3a (32532S/8242S/12829S, Cell Signaling, USA), HRP conjugated AffiniPure goat anti-rabbit (BA1055, BOSTER, Wuhan, China), PCR fluorescence quantification kit (Thermo Fisher, USA), Matrigel™ Matrix (BD Biosciences, USA), and $CD34^+$ positive selection cocktail (EasySep, Stemcell, Canada) were used in the experiments.

2.2. Establishment of COPD model with SD rat

All experimental animals were anesthetized before bleeding. Twenty-four SD male rats [(200±10) g body weight, obtained from Tianqin Biotechnology Co., Ltd. Changsha, China] were randomly divided into two groups (control and model group, 12 rats per group) in this study. The rats were kept under standard environmental conditions [(25±1)℃, 12 h light/dark cycle, and (55±5)% relative humidity]. The COPD rat model was established by the method of cigarette smoke combined with lipopolysaccharide (LPS) with reference to method reported by Nie *et al.*[16], and was improved to prolong the days of smoke exposure and the times of LPS infusion as following: Rats smoked passively twice a day (ten cigarettes each time, one hour each time). Rats were intratracheally injected with 0.2 mL (1 mg/mL) of LPS on days 30 and 45. On the 90th day, the rats were sacrificed by exsanguination of the abdominal aorta, and one side of the lung was lavaged to separate inflammatory cells from the lavage fluid. To determine whether the COPD model was successfully constructed, the remaining lung tissue was removed, sectioned, stained with HE, and observed under a light microscope (OLYMPUS BX53, Japan), while alveolar fusion and inflammation were analyzed.

2.3. EPC culture, identification, and grouping

COPD rats were sacrificed by exsanguination *via* the abdominal aorta. Arterial blood was collected and mononuclear cells were extracted by density gradient separation. The isolated mononuclear cells were enriched with a $CD34^+$ magnetic bead positive sorter, inoculated into a 6-well plate with EBM-2 medium (containing 10% fetal bovine serum), and then placed in a 37℃, 5% CO_2 incubator. After the fourth day of culture, the first liquid exchange was performed to remove the non-adherent cells. The medium was changed every 2 days, and the cells were identified on the 12th day. DiI-acLDL and FITC-UEA-I, with two types of fluorophores, were used for labeling, and DAPI was used for nuclear staining. Cells positive for all three colors were considered EPCs.

After successful isolation and culture of EPC, EPCs from the COPD group were divided into four groups: COPD group, PCDH-CMV-EF1-copGFP-Sirt1 transfection group, SRT1720 group, and EX527 group. The SRT1720 group was treated with SRT1720 (5 μM), and the EX527 group was treated with EX527 (1 μM). Then, the differences of proliferation, migration, adhesion, cell cycle, and apoptosis between different groups were compared. Sirt1 expression of COPD group and control group was detected by Western blotting and real-time PCR. The expression levels of Sirt1, FOXO3a, NF-κB, and p53 were also compared among COPD group, SRT1720 group, and EX527 group by Western blotting.

2.4. Lentivirus transfected EPC

A total of 4000 cells were inoculated into 96 well plates with 100 μL medium per well. One day later, PCDH-CMV-EF1-copGFP-Sirt1 lentivirus was added to co-culture with EPCs in fresh culture medium. Culture medium was replaced after 8 h, and GFP expression was detected by fluorescence microscope to determine whether the transfection was successful after 72 h.

2.5. EPC proliferation detection

Early-EPCs (10000/well) were seeded in 96 well-plates (Corning, USA) containing 100 μL EBM-2 medium (Lonza, USA) per well, containing 10% heat-inactivated fetal calf serum, 10% horse serum, stem cell growth factor (10 ng/mL; TEBU, Frankfurt, Germany), *L*-glutamine (2 mM) and vascular endothelial growth factor (5 ng/mL; TEBU, Sigma) in a humidified atmosphere (37℃, 5% CO_2). About 48 h to 72 h, the cells were in an exponential phase of growth and proliferated rapidly. The cell suspension to be tested was inoculated into a 96-well plate and cultured at 37℃ in a 5% CO_2 cell incubator for 24 h. CCK-8 solution was added to each well. The plate was then incubated in a CO_2 incubator for 3 h, and the absorbance at 450 nm was measured with a microplate reader (BioTek SynergyHTX, USA).

2.6. EPC migration detection

After adherent EPCs were trypsinized, the number of cells was adjusted to 10^4/mL with 1% fetal bovine serum basal medium, and 600 μL of basal medium was added to the lower chamber. Next, 200 μL of cell suspension was inoculated into the upper chamber of the transwell chamber. After 24 hours of culture, the chamber was removed and gently washed with 0.01% phosphate-buffered saline (PBS). The cells adhering to the chamber were removed, and the remaining cells were fixed with 4% paraformaldehyde for 10 min. The membrane at the bottom of the chamber was air-dried, stained with 0.1% crystal violet for 20 min, and observed under an inverted microscope (BioTek SynergyHTX, USA).

2.7. EPC adhesion detection

Digested cells were washed with PBS, resuspended in EBM-2 basal medium, and prepared into a suspension with a cell concentration of 10^4/mL. A total of 100 μL of cells were then seeded into a 96-well plate at 37℃ in a 5% CO_2 cell incubator. The cells were cultured for 30 min. The medium was aspirated, the cells were washed twice with PBS, and CCK-8 solution was added to each well to terminate cell growth. The plate was placed at 37℃and incubated in a 5% CO_2 incubator for 3 h. The number of adherent cells was observed and measured with a microplate reader (450 nm).

2.8. EPC cycle detection

EPCs were digested with trypsin, and the adherent cells were pipetted, collected in a 10-mL centrifuge tube, and centrifuged at 1000 *g* for 5 min to precipitate the cells. Precooled PBS was added. The cells were resuspended, transferred to a new 10-mL centrifuge tube, and pelleted by centrifugation. The supernatant was discarded. Next, 1 mL of precooled 75% ethanol was added. The suspension was mixed by blowing, and the cells were fixed at 4℃ for 24 h. After centrifugation at 1000 *g* for 5 min, the cells were pelleted. A total of 1 mL of precooled PBS was added. The cells were resuspended and the supernatant was removed by centrifugation. Propidium iodide staining solution (0.5 mL) was added to each sample tube. The cells were slowly resuspended, incubated at 37℃ for 30 min in the dark, and analyzed *via* flow cytometry.

2.9. EPC apoptosis detection

Cells were digested with trypsin without ethylene diamine tetraacetic acid, collected in a 10-mL centrifuge tube, and centrifuged at 2000 rpm for 5 min. The supernatant was removed. The cells were washed twice with PBS and then centrifuged at 2000 rpm for 5 min. The cells were suspended in 300 μL of 1×binding buffer, and 5 μL of annexin V-FITC was added. The suspension was mixed, protected from light, and incubated at room temperature for 15 min; 5 μL of PI staining solution was added 5 min before flow cytometry analysis.

2.10. Western blotting and real–time PCR

After the SDS-PAGE gel solidified, the glass plate was inserted into the electrophoresis tank. A 1×SDS-PAGE buffer was added. The comb was gently pulled out and the protein sample (40 μg) was added to the middle 4 wells. The electrophoresis tank was connected to the electrophoresis apparatus, and the voltage was adjusted to 75 V. After approximately 1 h, the protein loading buffer ran through the concentrated gel. The electrophoresis instrument was adjusted to 90 V, and the lower pressure gel was used for the lower layer. When the protein loading buffer ran to the bottom in 1 h, the power was turned off, and the electrophoresis was complete. The proteins were differentiated in 10% SDS-PAGE gels and transferred to PVDF membranes. The membrane was blocked with 5% skim milk for 1 h at room temperature and incubated overnight at 4℃ with primary antibodies (β-actin, Sirt1, p53, NF-κB, FOXO3a, 1:500) followed by incubation with HRP conjugated AffiniPure Goat Anti-rabbit secondary antibody (1:50) at 37℃ for 1 h. The membrane was then exposed with a gel imaging system using an ECL luminescence kit, and the exposed strips were measured for gradation using WCIF ImageJ v1.8.0 software.

Total RNA was extracted using the TRIzol method, and cDNA

was synthesized using a reverse transcription kit. Fluorescence quantitative PCR using PowerUp™ SYBR Green Master Mix was performed.

Conditions for qRT-PCR were as follows: 50℃ for 2 min, 95℃ for 2 min, 40 cycles at 95℃ for 5 s, 60℃ for 2 min. The relative quantification was calculated as a ratio of the target gene to reference gene by cycle threshold (Ct) values.

The *Sirt1*, *p53*, *NF-κB*, *FOXO3a* and internal reference (*GAPDH*) primers were designed with primer premier 3.0 software and synthesized by Sangon Biotech (Shanghai) Co., Ltd. The primer sequences are listed in Supplementary Table 1.

2.11. Immunofluorescence

The cell pellet was disrupted with a 4% paraformaldehyde fixation cassette and 0.2% Triton X-100 and then incubated with primary antibody at 4℃ overnight and secondary antibody for 1 h at room temperature in the dark. Finally, nuclei were counterstained with DAPI, and the expression of Sirt1 protein was observed under a laser confocal microscope (OLYMPUS FV1000, Japan).

2.12. Statistical analysis

Statistical analysis was performed with SPSS20.0. Results were presented as mean ± standard deviation (SD). One-way analysis of variance (ANOVA) was used for multigroup comparison, and student *t* test was used for comparison beween two groups. A value of $P<0.05$ was considered statistically significant.

2.13. Ethical statement

All the protocols performed in this study were approved by the Ethics Committee of Hainan Medical College (HYLL-2014-30) and complied with the rules of the NIH for the animal ethics of Laboratory Animals (NIH Publication 80-23, 1996).

3. Results

3.1. Successful establishment of COPD rat model

After SD rats were sacrificed by bloodletting, the lungs of SD rats were resected for observation. The lung tissue from the model group was significantly enlarged compared with that from the control group. The appearance was bright, the edge was round, and fine black particles were observed on the surface of the lung. Pathological lung tissue sections were observed under a light microscope. The alveolar structure in lungs from the model group was destroyed and fused, and the air cavity was enlarged. A large number of infiltrated inflammatory cells were observed. In the control group, the structures of bronchioles, alveolar ducts, and alveolar spaces were intact and clear. No epithelial cells were detached, no thickening was observed in the wall, and the alveolar spaces were thick. The cell count in alveolar lavage fluid from the model group [$(91\pm11)\times10^4$/mL] was found to be significantly increased compared with that in the control group [$(23\pm5)\times10^4$/mL]. All these results indicated that the COPD model was successfully established (Supplementary Figure 1).

3.2. EPC proliferation, adhesion, migration

After COPD rat model was successfully established, EPCs were separated and cultured. The newly isolated mononuclear cells were round in shape under an inverted phase contrast microscope. After 3 d, the adherent cells began to stretch and appeared spindle-shaped. After 7 d, some cells had formed colonies, and the spindle cells were seen to grow from the edge of the colony. Visible paving stone-like cells grew after 12 d. After labeling with DiI-acLDL, FITC-UEA-I and DAPI, the cells positive for the three stains were observed to be differentiated EPCs under laser confocal microscopy (Supplementary Figure 2).

EPCs grew logarithmically during 48-72 h, but the growth of cells in the COPD group was significantly lower than that in the control group. The cell proliferation ability was significantly lower than that in the control group ($P<0.05$) (Figure 1A). The adhesion (Figure 1B) and migration (Figure 1C, D) ability were significantly lower than that in the control group ($P<0.05$) (Supplementary Table 2).

3.3. EPC cycle determination

EPCs in the COPD group were mostly in the G_0G_1 phase, while the percentage of EPCs in the S phase and G_2M phase was significantly reduced ($P<0.05$). The replication ability of EPCs in peripheral blood of the COPD group was significantly lower than that of cells in the control group ($P<0.05$) (Figure 2, Supplementary Table 3).

3.4. EPC apoptosis assay

The apoptosis rate of EPCs from peripheral blood in the COPD group was significantly higher than that in the control group based on flow cytometry analysis ($P<0.05$) (Figure 3, Supplementary Table 3).

3.5. Expression of Sirt1 in EPCs

The expression of Sirt1 in EPCs was detected with an immunofluorescence assay. The results showed that Sirt1 was expressed in both the control and COPD groups. The expression

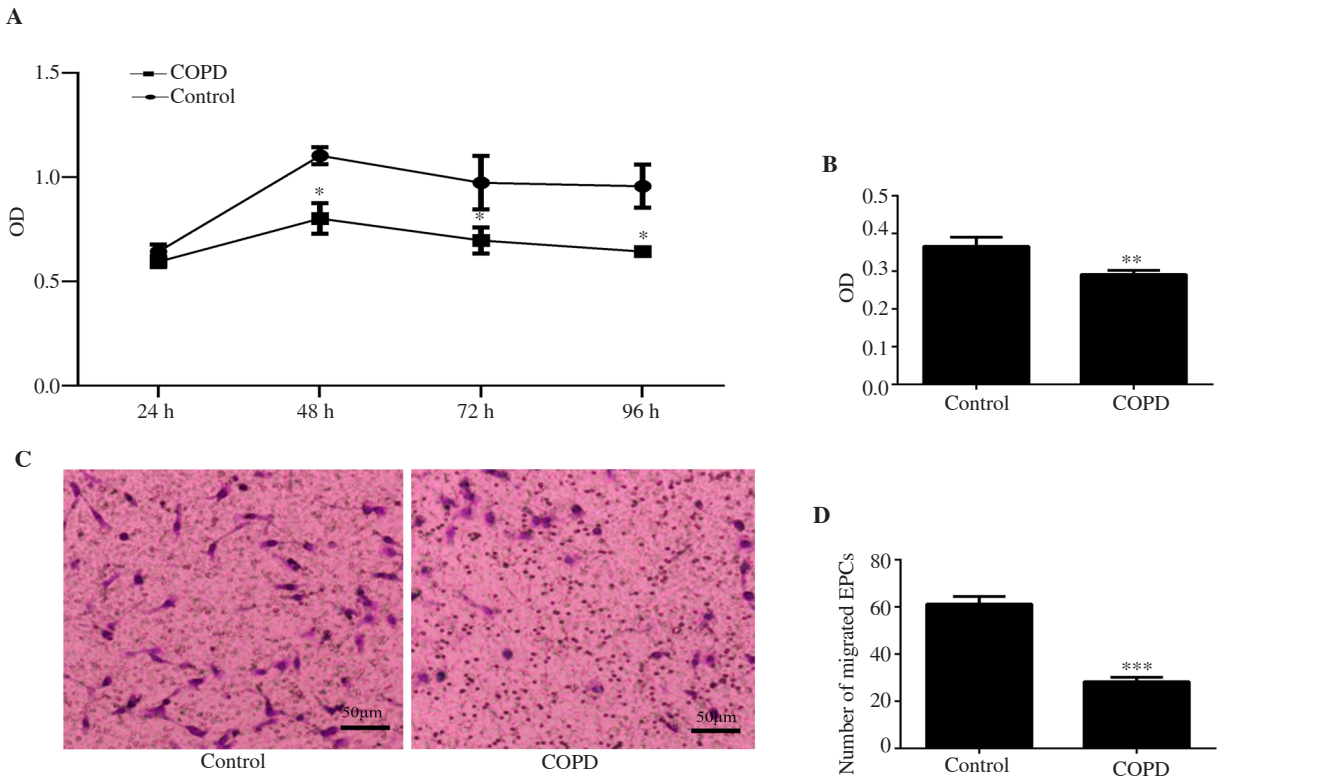

Figure 1. (A) Endothelial progenitor cells (EPCs) proliferation. (B) EPC adhesion. (C) Migration of chronic obstructive pulmonary disease (COPD) and control EPCs under the inverted microscope. (D) Number of migrated EPCs. The proliferation, adhesion, and migration of EPCs in the COPD group were significantly lower than those in the control group. n=8, mean±SD; $^{*}P$<0.05, $^{**}P$<0.01, $^{***}P$<0.001. Bar: 50 μm.

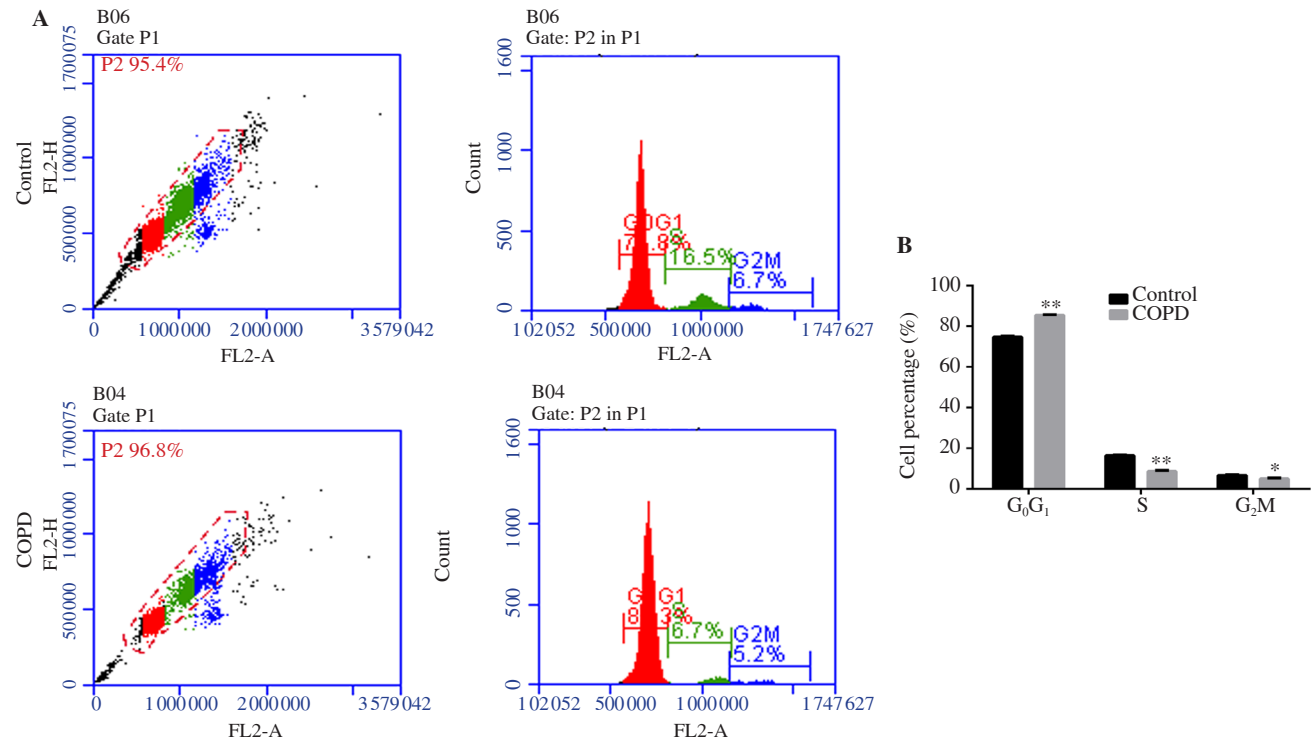

Figure 2. Cell cycle of EPCs. (A) Flow cytometry result. (B) Percentage of EPCs in different cell cycle. EPCs in the COPD group were mostly in G_0G_1 phase, while the number of EPCs in S phase and G_2M phase was significantly reduced. n=8, mean±SD; $^{*}P$<0.05, $^{**}P$<0.01.

.

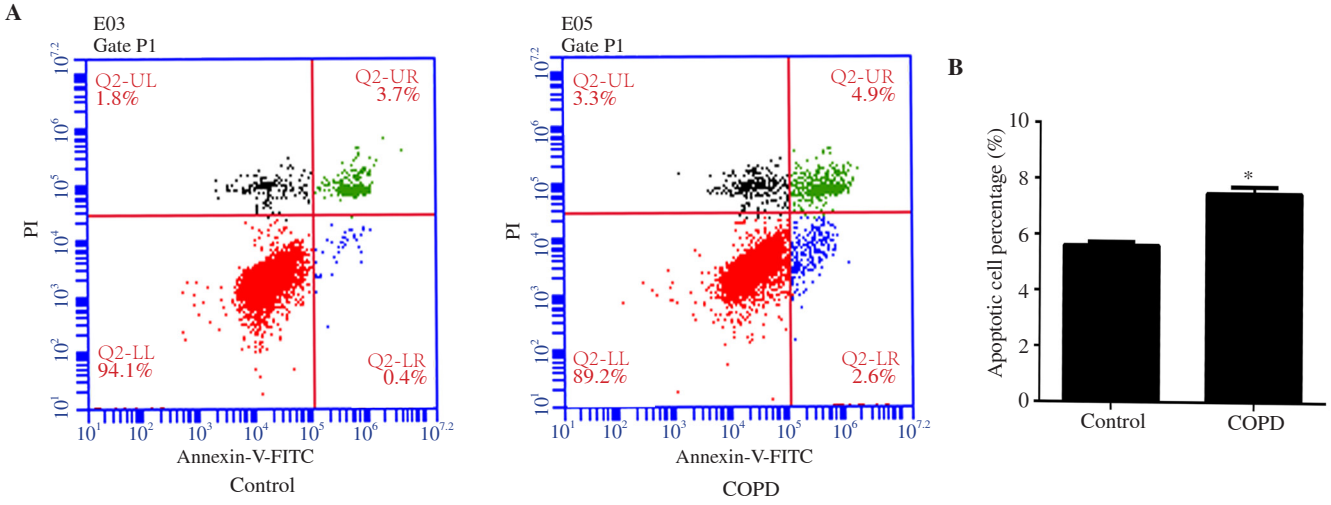

Figure 3. Apoptosis of EPCs. (A) Flow cytometry result. (B) Percentage of apoptotic EPCs. The percentage of apoptotic EPCs from peripheral blood in the COPD group was significantly higher than that in the control group. n=8, mean±SD; $^{*}P$<0.05.

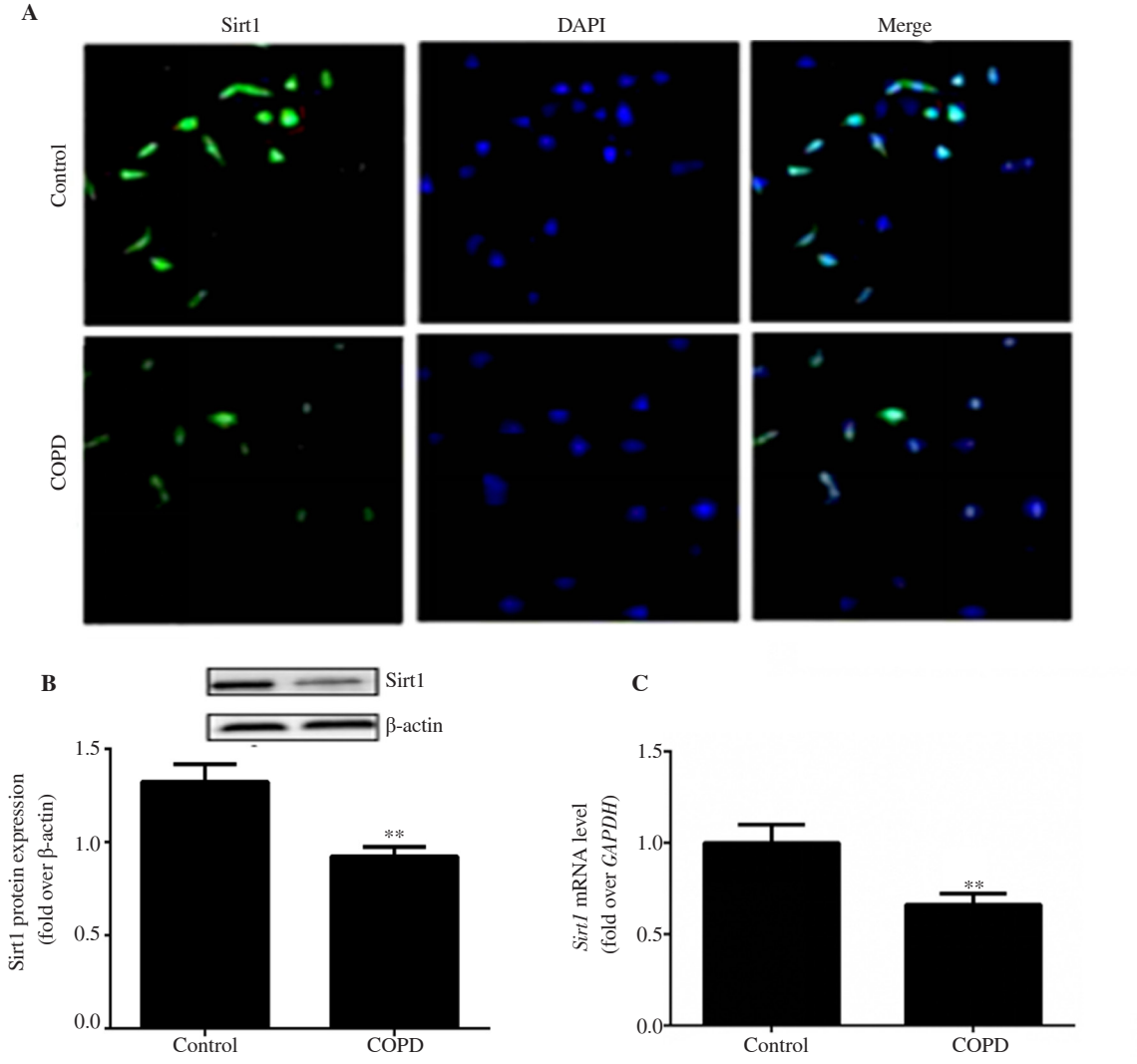

Figure 4. Expression of Sirt1 in EPCs. (A) Immunofluorescence observation of Sirt1 expression in EPCs (10×20). (B) Sirt1 protein expression in EPCs. (C) *Sirt1* mRNA level in EPCs. n=8, mean±SD, $^{**}P$<0.01. Bar: 50 μm.

of Sirt1 in EPCs of the COPD group was lower than that in the control group. The results of Western blotting and real-time PCR also showed that Sirt1 expression in EPCs of the COPD group was significantly lower (P<0.01) (Figure 4).

3.6. Sirt1 overexpression, SRT1720, EX527 affect proliferation, adhesion, and migration functions of EPC in COPD

EPCs were transduced with PCDH-CMV-EF1-copGFP-Sirt1 and observed under a fluorescence microscope. After 3 d, green fluorescence was observed, and the transduction rate was over 80% (Figure 5A). The adhesion ability of EPCs in the SRT1720 group was significantly higher than that in the COPD group (P<0.01), while there was no significant difference between the COPD group and the EX527 group (Figure 5B). The proliferative capacity of EPCs in the lentiviral transduction group was significantly higher than that in the COPD group at 24 h. The proliferation of EPCs in the SRT1720 (agonist) group was significantly higher than that in the COPD group (P<0.05). The proliferation of COPD EPCs in the EX527 (inhibitor) group was significantly lower than that in the COPD group (P<0.01) (Figure 5C). There was no significant difference in the proliferation ability of EPCs between the SRT1720 group and the lentiviral transduction group. The migration ability of EPCs in the SRT1720 group was significantly higher than that of cells in the COPD group based on transwell assays (P<0.001), and the migration ability of EPCs in the EX527 group was significantly lower than that of cells in the COPD group at 24 h (Figure 5D, E) (P<0.01) (Supplementary Table 4, 5).

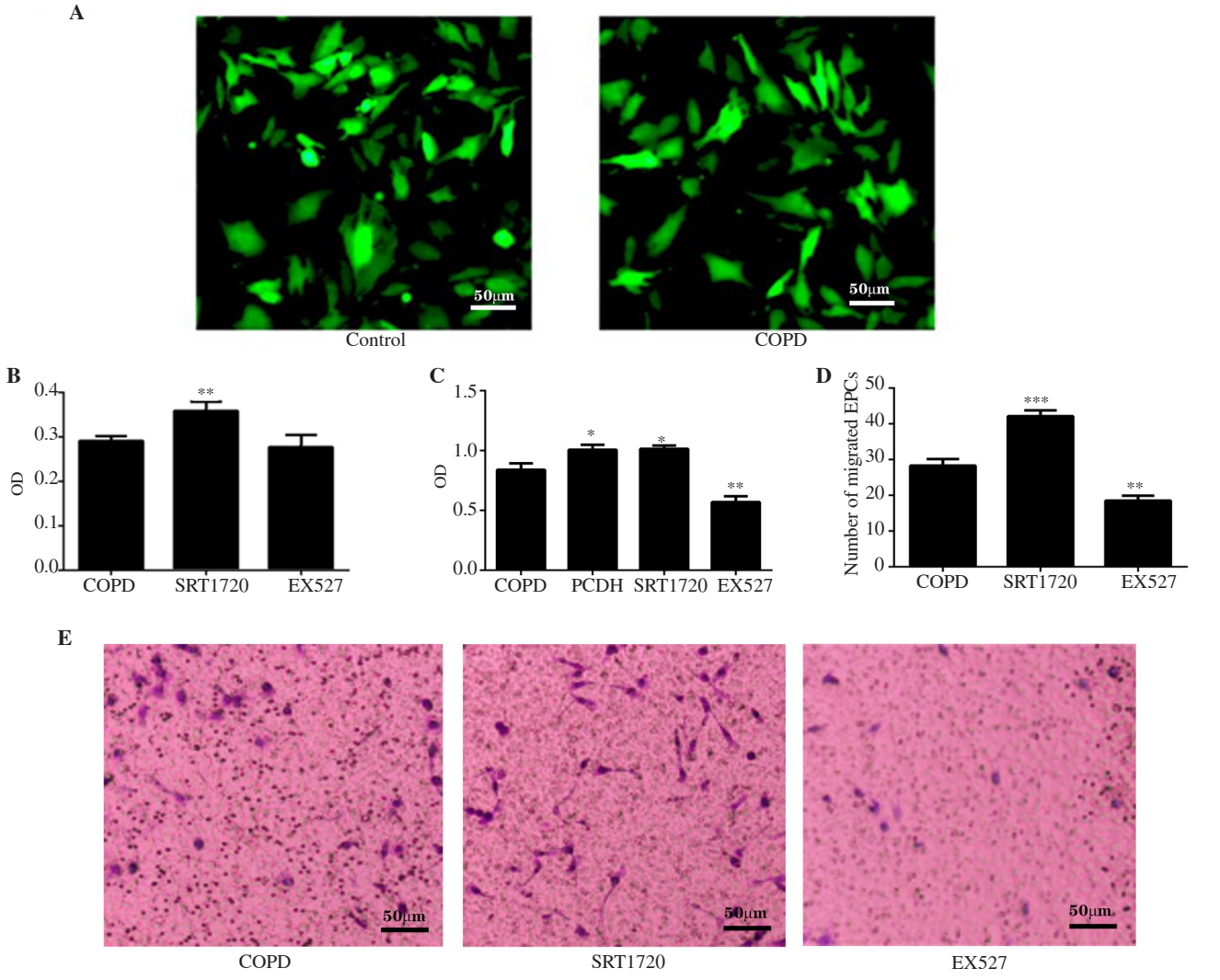

Figure 5. Effect of Sirt1 expression on the function of EPCs. (A) EPC transduction with PCDH-CMV-EF1-copGFP-Sirt1(10×40). (B) EPCs adhesion. (C) EPC proliferation. (D) Number of migrated EPCs. (E) Migration of EPC under inverted microscope. EPCs were transduced successfully. SRT1720 promotes EPC adhesion, proliferation and migration of COPD, and EX527 inhibits their adhesion, proliferation and migration. Overexpression of Sirt1 promotes EPC proliferation of COPD. n=8, mean±SD; $^{*}P$<0.05, $^{**}P$<0.01, $^{***}P$<0.001. Bar: 50 μm. PCDH: PCDH-CMV-EF1-copGFP-Sirt1.

3.7. SRT1720 and EX527 affect the EPC cell cycle of COPD

The percentage of EPCs cells in the G_0G_1 phase in the SRT1720 group was significantly reduced compared with that in the COPD group (P<0.01), and the percentage of EPCs in the S phase and G_2M phase was significantly increased (P<0.05). The proportion of EPCs in the G_0G_1 phase of the EX527 group was significantly increased compared with that in the COPD group (P<0.05), and the percentage of EPCs in the G_2M phase decreased (Figure 6, Supplementary Table 6) .

3.8. SRT1720 and EX527 affect the EPC apoptosis of COPD

The number of apoptotic EPCs cells in the SRT1720 group was significantly lower than that in the COPD group (P<0.05), and the number of EPCs in the EX527 group was significantly higher than that in the COPD group (P<0.01) (Figure 7, Supplementary Table 6).

3.9. Effect of Sirt1 expression on FOXO3a , NF-κB and p53

The results showed that, compared with that in the COPD group, both mRNA and protein expressions of Sirt1 and FOXO3a in EPCs were significantly increased in the SRT1720 group (P<0.05), while p53 and NF-κB levels were decreased. At the same time, the mRNA expressions of FOXO3a and Sirt1 as well as protein expression of FOXO3a in EPCs in the EX527 group were significantly decreased (P<0.05), while p53 and NF-κB levels were increased except p53 mRNA level, and the increase of NF-κB protein level was not significant (Figure 8).

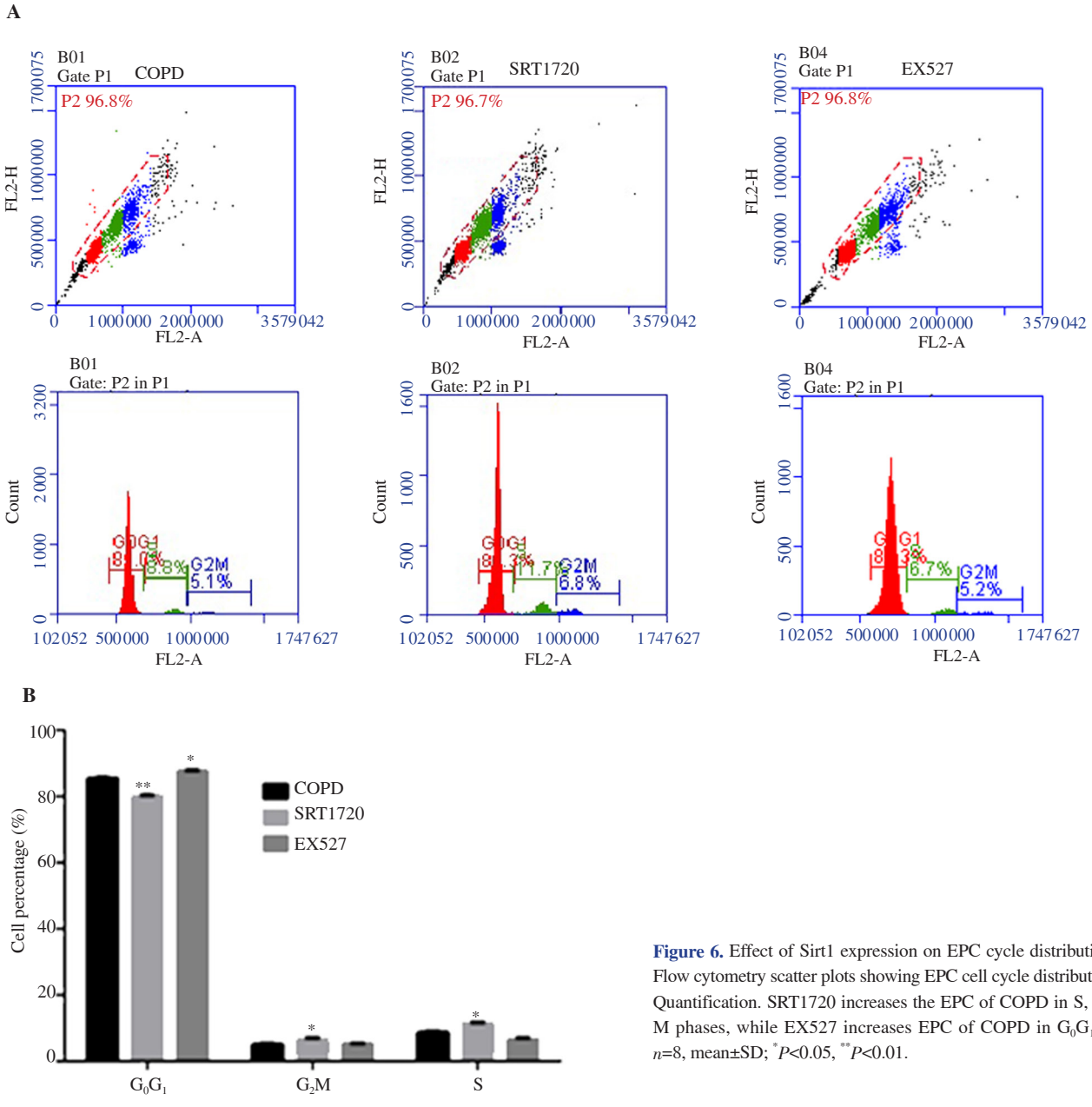

Figure 6. Effect of Sirt1 expression on EPC cycle distribution. (A) Flow cytometry scatter plots showing EPC cell cycle distribution. (B) Quantification. SRT1720 increases the EPC of COPD in S, G_2, and M phases, while EX527 increases EPC of COPD in G_0G_1 phase. n=8, mean±SD; $^*P$<0.05, $^{**}P$<0.01.

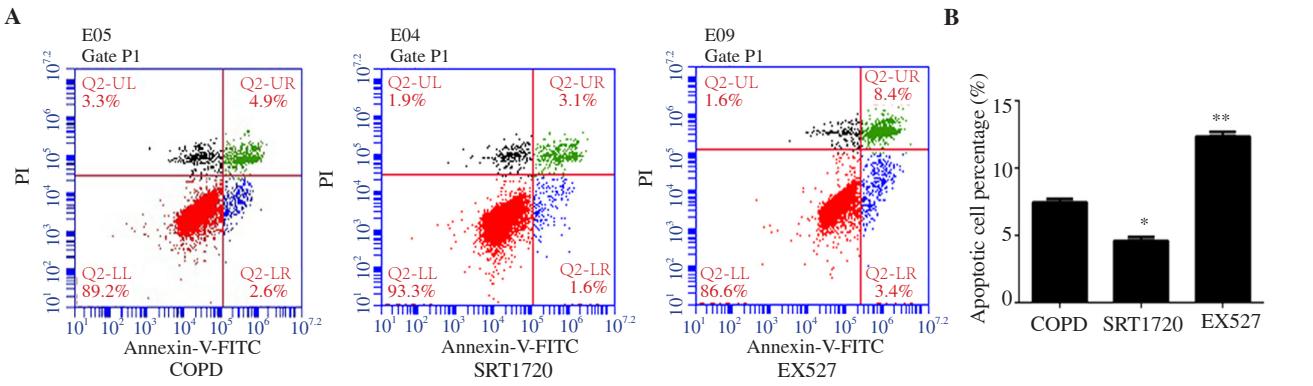

Figure 7. Effect of Sirt1 expression on apoptosis of EPCs. (A) Flow cytometry scatter plots showing the proportion of apoptotic cells. (B) Quantification of apoptosis. SRT1720 reduces EPC apoptosis of COPD, while EX527 promotes EPC apoptosis of COPD. n=8, mean±SD; $^{*}P$<0.05, $^{**}P$<0.01.

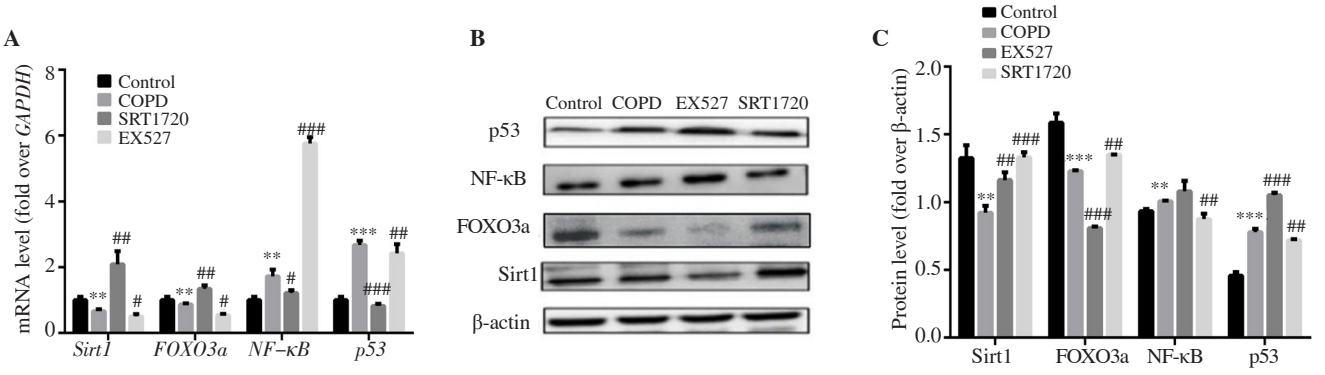

Figure 8. (A) mRNA expression. (B) Western blotting result. (C) Protein expression. n=3, mean±SD; $^{**}P$<0.01, $^{***}P$<0.001 *vs.* control; $^{\#}P$<0.05, $^{\#\#}P$<0.01, $^{\#\#\#}P$<0.001 *vs.* COPD.

4. Discussion

Smoking is the main risk factor for COPD[17]. In this study, the model of COPD was established by fumigation combined with LPS administration. The rat model was successfully constructed based on the observation of alveolar lavage fluid and pathological staining.

After the successful construction of the COPD rat model, the abdominal aortic blood was extracted, and EPCs were separated by density gradient centrifugation. The proliferation, adhesion, and migration ability of the isolated EPCs were significantly lower than that of control group cells, and these results were consistent with previous researches[18]. The number of cells in the G_0/G_1 phase increased significantly; however, the number of cells in the S phase and G_2/M phase was significantly decreased. This indicated that the proliferation of EPCs decreased. The number of apoptotic EPCs in the COPD group was significantly higher than that in the control group. Therefore, it is speculated that dysfunctional EPCs were present in the COPD group. The proliferation, adhesion, and migration of EPCs decreased, and apoptosis increased, which led to a decrease in the number of EPCs in peripheral blood from the COPD group.

Sirt1 is closely related to COPD[19]. The expression of Sirt1 in alveolar macrophages and bronchial epithelial cells is downregulated by smoking; Sirt1 activity is decreased, and the interaction of Sirt1 with certain inflammatory factors is disrupted[20]. The expression of Sirt1 was found to be decreased in COPD animal models and in lung tissue from COPD patients and smokers[21,22], which was consistent with the results of this study.

It was reported that overexpression of Sirt1 might be able to promote the proliferation, decrease the apoptosis of HK-2 cells and protect the cells from the damage caused by LPS-induced acute kidney injury[23]. In our study, the number of apoptotic EPCs from PCDH-CMV-EF1-copGFP-Sirt1 lentivirus and Sirt1 agonist (SRT1720) group was decreased. Their proliferation, adhesion, and migration ability were enhanced because of the increased Sirt1 expression. However, the Sirt1 expression in EPCs of COPD rats was lower than that of control, leading to apoptosis of EPCs. It was partly explained why the number of EPCs in peripheral blood was decreased in COPD rats; on the other side, the cell cycle of EPCs from COPD rats was arrested due to the low level of Sirt1 expression. The same result was found in EX527 (inhibitor) applied group. The number of cells in the G_0G_1 phase was significantly reduced, and the number of apoptotic cells was significantly smaller than in previous reports[24,25]. It was concluded that the increase in Sirt1 expression in EPCs in peripheral blood of COPD rats can promote EPC proliferation, migration, and adhesion, reduce apoptosis, enhance the repair function of EPCs.

Sirt1 plays an important role in apoptosis resistance, oxidative stress, and inflammation[26,27]. Sirt1 deacetylates histones and nonhistones. Through deacetylation, certain transcriptional regulatory factors, such as a forkhead transcription factor (FOXO3a), tumor transcription factor (p53), and nuclear transcription factor (NF-κB), are involved in oxidative stress, cell cycle, apoptosis, and inflammatory responses[28-30]. The results of this experiment showed that the expression level of Sirt1 was decreased in EPCs, the degree of deacetylation of FOXO3a was decreased, and apoptosis was increased. Due to decreased expression of Sirt1, p53 was highly acetylated, inducing apoptosis of EPCs. The number of apoptotic EPCs increased could partly be explained by enhanced p53 and NF-κB activity[31]. Interestingly, the change trend of protein levels were not completely consistent with their mRNA levels in our experiment. This shows that EX527 may also affect the mRNA or protein half-life *via* some mechanism when acting on EPC cells in COPD. Therefore, we hypothesize that the decreased expression of Sirt1 increases inflammation by promoting NF-κB, impaires DNA repair by deactivating FOXO3a, and reduces cell survival through the induction of p53 in COPD.

A major limitation of the present study is the COPD model. Most studies established the model of SD rats by cigarette smoke (CS), intratracheal LPS, and intranasal elastase[32,33]. However, there is currently no uniform standard for the evaluation of animal models. The evaluation parameters used in most studies are mainly lung pathological indicators and pulmonary inflammation parameters (inflammatory cells and inflammatory mediators). We did not measure cytokine levels in this experiment, which is the limit of our study. Besides, the effects of the blockade of the related signaling pathways were not assessed. In future studies, we will block the Sirt1-FOXO3a and Sirt1-NF-κB signaling pathways to observe the resulting functional changes in EPCs to find a feasible solution for improving the function of EPCs in peripheral blood of COPD patients.

Conflict of interest statement

The authors declare no conflict of interest.

Acknowledgments

We thank Guo-Hui Yi, Li-Min Zhou for technical assistance, and also thank Shan-Xia Liu, Sheng-Nan Tian, Yi-Ying Zheng, and the staff of the Central Laboratory of Hainan Medical College. Our project has also partially supported by Hainan Clinical Medical Center, China, we express our appreciation for their funding.

Funding

It is supported by NSCF (No. 81260010,81460006 and 81660011) and Hainan Natural Science Fund (No. 20168264, 817134).

Authors' contributions

XL conceived the concepts; XL and YS designed the study; DS, JY, ZD, JQ, and QH performed experiments; DS, JY, and ZD performed data analysis, statistical analysis and original manuscript preparation; XL and YS edited and reviewed manuscript.

References

[1] GBD Chronic Respiratory Disease Collaborators. Prevalence and attributable health burden of chronic respiratory diseases, 1990-2017: A systematic analysis for the Global Burden of Disease Study 2017. *Lancet Respir Med* 2020; **8**(6): 585-596.

[2] GBD 2017 Causes of Death Collaborators. Global, regional, and national age-sex-specific mortality for 282 causes of death in 195 countries and territories, 1980–2017: A systematic analysis for the Global Burden of Disease Study 2017. *Lancet* 2018; **392**(10159): 1736-1788.

[3] Fang L, Gao P, Bao H, Tang X, Wang B, Feng Y, et al. Chronic obstructive pulmonary disease in China: A nationwide prevalence study. *Lancet Respir Med* 2018; **6**(6): 421-430.

[4] Rabe KF, Watz H. Chronic obstructive pulmonary disease. *Lancet* 2017; **389**(10082): 1931-1940.

[5] Singh D, Agusti A, Anzueto A, Barnes PJ, Bourbeau J, Celli BR, et al. Global strategy for the diagnosis, management, and prevention of chronic obstructive lung disease: The GOLD science committee report 2019. *Eur Respir J* 2019; **53**(5): 1900164.

[6] Morgan AD, Rothnie KJ, Bhaskaran K, Smeeth L, Quint JK. Chronic obstructive pulmonary disease and the risk of 12 cardiovascular diseases: A population-based study using UK primary care data. *Thorax* 2018; **73**(9): 877-879.

[7] Güven H, Shepherd RM, Bach RG, Capoccia BJ, Link DC. The number of endothelial progenitor cell colonies in the blood is increased in patients with angiographically significant coronary artery disease. *J Am Coll Cardiol* 2006; **48**(8): 1579-1587.

[8] Palange P, Testa U, Huertas A, Calabrò L, Antonucci R, Petrucci E, et al. Circulating haemopoietic and endothelial progenitor cells are decreased in COPD. *Eur Respir J* 2006; **27**(3): 529-541.

[9] Takahashi T, Suzuki S, Kubo H, Yamaya M, Kurosawa S, Kato M. Impaired endothelial progenitor cell mobilization and colony-forming capacity in chronic obstructive pulmonary disease. *Respirology* 2011; **16**(4): 680-687.

[10] Yue WS, Wang M, Yan GH, Yiu KH, Yin L, Lee SW, et al. Smoking is associated with depletion of circulating endothelial progenitor cells and elevated pulmonary artery systolic pressure in patients with coronary artery disease. *Am J Cardiol* 2010; **106**(9): 1248-1254.

[11]Liu X, Tan W, Liu Y, Tan W, Liu Y, Lin G, et al. The role of the β2AR on EPCs dysfunction of proliferation and migration in COPD patients. *Expert Opin Ther Targets* 2013; **17**(5): 485-500.

[12]Finkel T, Deng CX, Mostoslavsky R. Recent progress in the biology and physiology of sirtuins. *Nature* 2009; **460**(7255): 587-591.

[13]Liu X, Tan W, Liu Y, Lin G, Xie C. Protective effects of resveratrol on postmenopausal osteoporosis: Regulation of Sirt1-NF-κB signaling pathway. *Acta Biochim Biophys Sin (Shanghai)* 2014; **46**(12): 1024-1033.

[14]Rajendrasozhan S, Yang SR, Kinnula VL, Rahman I. SIRT1, an antiinflammatory and antiaging protein, is decreased in lungs of patients with chronic obstructive pulmonary disease. *Am J Respir Crit Care Med* 2008; **177**(8): 861-870.

[15]Yao H, Sundar IK, Ahmad T, Lerner C, Gerloff J, Friedman AE, et al. SIRT1 protects against cigarette smoke-induced lung oxidative stress *via* a FOXO3-dependent mechanism. *Am J Physiol Lung Cell Mol Physiol* 2014; **306**(9): L816-L828.

[16]Nie YC, Wu H, Li PB, Luo YL, Zhang CC, Shen JG, et al. Characteristic comparison of three rat models induced by cigarettesmoke or combined with LPS: To establish a suitable model forstudy of airway mucus hypersecretion in chronic obstructive pulmonary disease. *Pulm Pharmacol Ther* 2012; **5**(5): 349-356.

[17]Malerba M, Montuschi P. Non-invasive biomarkers of lung inflammation in smoking subjects. *Curr Med Chem* 2012; **19**(2): 187-196.

[18]Liu X, Xie C. Human endothelial progenitor cells isolated from COPD patients are dysfunctional. *Mol Cell Biochem* 2012; **363**(1-2): 53-63.

[19]Sadarani BN, Majumdar AS. Resveratrol potentiates the effect of dexamethasone in rat model of acute lung inflammation. *Int Immunopharmacol* 2015; **28**(1): 773-779.

[20]Caito S, Hwang JW, Chung S, Yao H, Sundar IK, Rahman I. PARP-1 inhibition does not restore oxidant-mediated reduction in Sirt1 activity. *Biochem Biophys Res Commun* 2010; **392**(3): 264-270.

[21]Conti V, Corbi G, Manzo V, Malangone P, Vitale C, Maglio A, et al. SIRT1 activity in peripheral blood mononuclear cells correlates with altered lung function in patients with chronic obstructive pulmonary disease. *Oxid Med Cell Longev* 2018; **2018**: 9391261.

[22]Guan R, Wang J, Cai Z, Li Z, Wang L, Li Y, et al. Hydrogen sulfide attenuates cigarette smoke-induced airway remodeling by upregulating SIRT1 signaling pathway. *Redox Biol* 2020; **28**: 101356.

[23]Gao Q, Zhu H. The overexpression of Sirtuin1 (SIRT1) alleviated lipopolysaccharide (LPS)-induced acute kidney injury (AKI) *via* inhibiting the activation of nucleotide-binding oligomerization domain-like receptors (NLR) family pyrin domain containing 3 (NLRP3) inflammasome. *Med Sci Monit* 2019; **25**: 2718-2726.

[24]Tao A, Xu X, Kvietys P, Kao R, Martin C, Rui T. Experimental diabetes mellitus exacerbates ischemia/reperfusion-induced myocardial injury by promoting mitochondrial fission: Role of down-regulation of myocardial Sirt1 and subsequent Akt/Drp1 interaction. *Int J Biochem Cell Biol* 2018; **105**: 94-103.

[25]Ming GF, Wu K, Hu K, Chen Y, Xiao J. NAMPT regulates senescence, proliferation, and migration of endothelial progenitor cells through the SIRT1 AS lncRNA/miR-22/SIRT1 pathway. *Biochem Biophys Res Commun* 2016; **478**(3): 1382-1388.

[26]Chan SH, Hung CH, Shih JY, Chu PM, Cheng YH, Lin HC, et al. SIRT1 inhibition causes oxidative stress and inflammation in patients with coronary artery disease. *Redox Biol* 2017; **13**: 301-309.

[27]Oza MJ, Kulkarni YA. Formononetin alleviates diabetic ccardiomyopathy by inhibiting oxidative stress and upregulating SIRT1 in rats. *Asian Pac J Trop Biomed* 2020; **10**(6): 254-262.

[28]Du C, Lin X, Xu W, Zheng F, Cai J, Yang J, et al. Sulfhydrated Sirtuin-1 increasing its deacetylation activity is an essential epigenetics mechanism of anti-atherogenesis by hydrogen sulfide. *Antioxid Redox Signal* 2019; **30**(2): 184-197.

[29]Xu K, Liu S, Zhao X, Zhang X, Fu X, Zhou Y, et al. Treating hyperuricemia related non-alcoholic fatty liver disease in rats with resveratrol. *Biomed Pharmacother* 2019; **110**: 844-849.

[30]Sabitha R, Nishi K, Gunasekaran VP, Annamalai G, Agilan B, Ganeshan M. *p*-Coumaric acid ameliorates ethanol-induced kidney injury by inhibiting inflammatory cytokine production and NF-κB signaling in rats. *Asian Pac J Trop Biomed* 2019; **9**(5): 188-195.

[31]Tang H, Li K, Zhang S, Lan H, Liang L, Huang C, et al. Inhibitory effect of paeonol on apoptosis, oxidative stress, and inflammatory response in human umbilical vein endothelial cells induced by high glucose and palmitic acid induced through regulating SIRT1/FOXO3a/NF-kappaB pathway. *J Interferon Cytokine Res* 2021; **41**(3): 111-124.

[32]Jones B, Donovan C, Liu G, Gomez HM, Chimankar V, Harrison CL, et al. Animal models of COPD: What do they tell us? *Respirology* 2017; **22**(1): 21-32.

[33]Ghorani V, Boskabady MH, Khazdair MR, Kianmeher M. Experimental animal models for COPD: A methodological review. *Tob Induc Dis* 2017; 15: 25.

Title of the article: Effects of Sirt1 on Proliferation, Migration and Apoptosis of Endothelial Progenitor Cells in Peripheral Blood of SD Rats with Chronic Obstructive Pulmonary Disease

First author: Dong-Mei Sun, The First Affiliated Hospital of Hainan Medical University

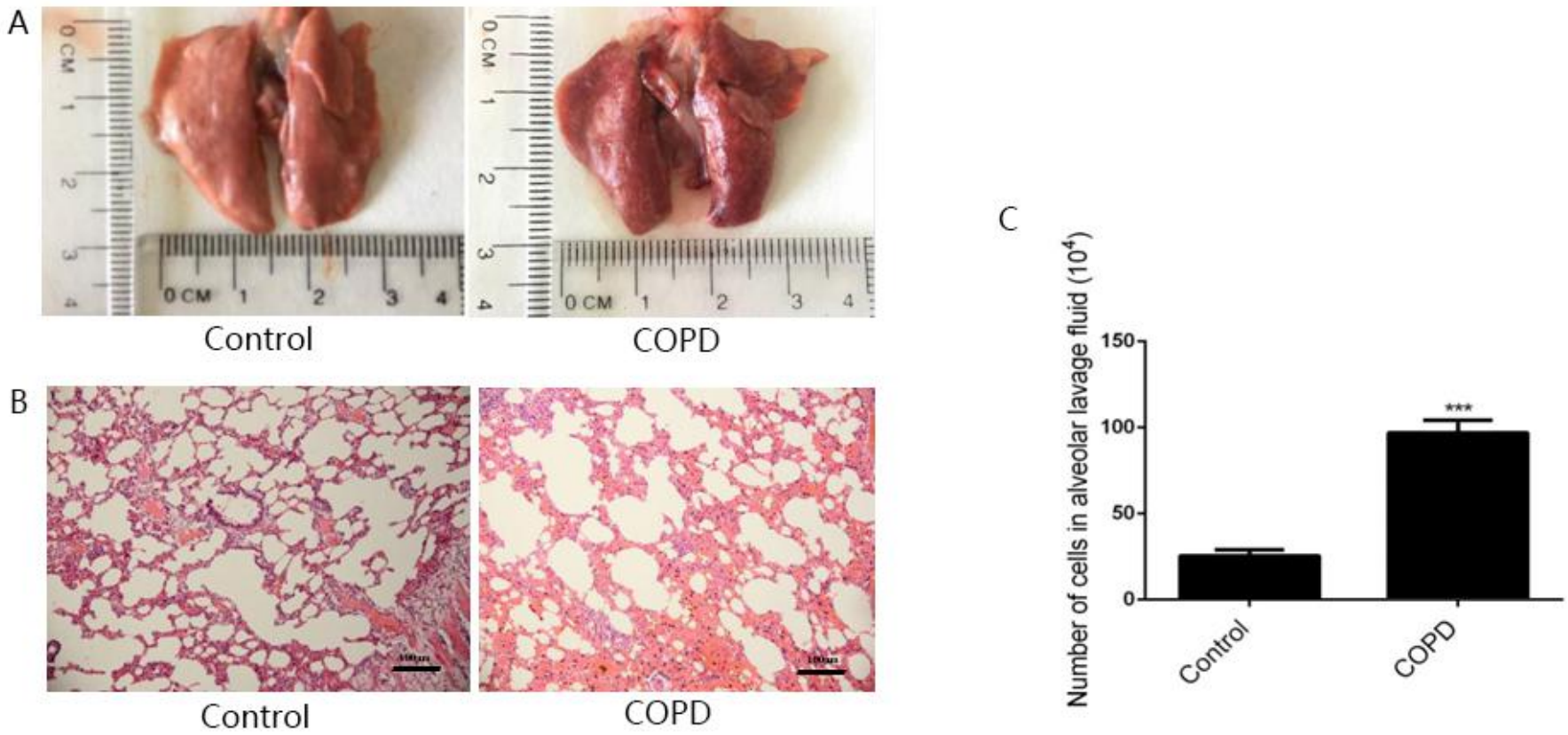

Suppl Figure 1. COPD rat model establishment. (A) The lung tissue from the model group was significantly enlarged compared with that from the control group, and the appearance was bright, the edge was round, and fine black particles were observed on the surface of the lung (n=8,`x±s, $^{***}P<0.001$); (B) H&E staining of lung tissue (10× 20); (C) Inflammatory cell count in bronchoalveolar lavage fluid control. The cell count in alveolar lavage fluid from the model group was significantly increased compared with that in the control group (Control: $23±5×10^4$/ml COPD: $91±11×10^4$/ml)

Title of the article: Effects of Sirt1 on Proliferation, Migration and Apoptosis of Endothelial Progenitor Cells in Peripheral Blood of SD Rats with Chronic Obstructive Pulmonary Disease

First author: Dong-Mei Sun, The First Affiliated Hospital of Hainan Medical University

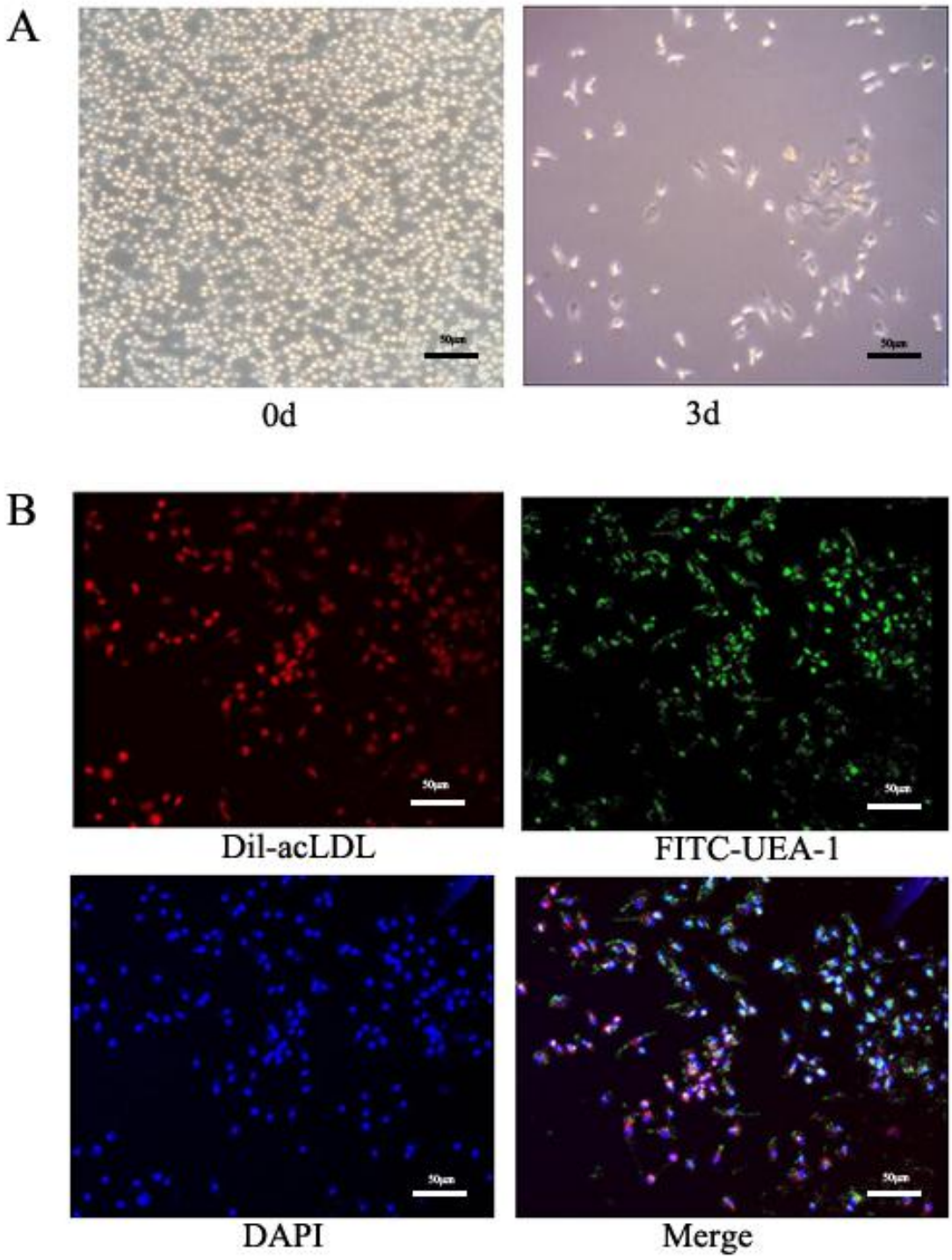

Suppl Figure 2. Identification of endothelial progenitor cells. (A) Mononuclear cells were isolated as small rounds and were cultured for 3-4 days; (B) Dil-acLDL (red) and FITC-UEA-I (green) staining, DAPI staining, and EPCs (tricolor-positive cells). After labeling with DiI-acLDL, FITC-UEA-I and DAPI, the cells positive for the three stains were observed to be differentiated EPCs via laser confocal microscopy. (10×20).

Title of the article: Effects of Sirt1 on Proliferation, Migration and Apoptosis of Endothelial Progenitor Cells in Peripheral Blood of SD Rats with Chronic Obstructive Pulmonary Disease

First author: Dong-Mei Sun, The First Affiliated Hospital of Hainan Medical University

Suppl Table 1. Primer sequences used for quantitative real-time PCR.

Name	Primer sequence （5’-3’）	Product （bp）
GAPDH	FORWARD: CTGCACCACCAACTGCTTA REVERSE: GCCATCCACAGTCTTCTGA	120
Sirt1	FORWARD: TTCCAGCCATCTCTGTGTCA REVERSE: GATCCTTTGGATTCCTGCAA	117
FOXO3a	FORWARD: CATGCAGACCATCCAGGAGA REVERSE: ATGACATCGCTGTGGCTGAG	114
NF-κB	FORWARD: CTGGTGCATTCTGACCTTGC REVERSE: GGTCCATCTCCTTGGTCTGC	118
P53	FORWARD: ACCAGCACAAGCTCCTCTCC REVERSE: AAGGCCTCATTCAGCTCTCG	116

Title of the article: Effects of Sirt1 on Proliferation, Migration and Apoptosis of Endothelial Progenitor Cells in Peripheral Blood of SD Rats with Chronic Obstructive Pulmonary Disease

First author: Dong-Mei Sun, The First Affiliated Hospital of Hainan Medical University

Suppl Table 2. Proliferation, adhesion and migration detection of EPCs. (A450 nm)

	Proliferation (OD)	Adhesion (OD)	Number of migratory EPCs
Control	1.103 ± 0.041	0.349 ± 0.034	59±4.5
COPD	0.8020 ± 0.073*	0.284 ± 0.015**	27±2.6****

*P<0.05, **P<0.01, ***P<0.001, ****P<0.0001

Title of the article: Effects of Sirt1 on Proliferation, Migration and Apoptosis of Endothelial Progenitor Cells in Peripheral Blood of SD Rats with Chronic Obstructive Pulmonary Disease

First author: Dong-Mei Sun, The First Affiliated Hospital of Hainan Medical University

Suppl Table 3. The proportion of cells in each cell cycle phase and proportion of apoptotic cells. (%, n=3, $\bar{x}$±s)

	G_0G_1	G_2M	S	Apoptosis
Control	74.4±0.57	6.4±0.50	16.3±0.35	4.1±0.1
COPD	85.3±0.35**	4.8±0.50*	8.4±0.57**	7.5±0.3*

***P<0.05, ****P<0.01**

Title of the article: Effects of Sirt1 on Proliferation, Migration and Apoptosis of Endothelial Progenitor Cells in Peripheral Blood of SD Rats with Chronic Obstructive Pulmonary Disease

First author: Dong-Mei Sun, The First Affiliated Hospital of Hainan Medical University

Suppl Table 4. Proliferation ditection of EPCs.(A450 nm)

	OD
COPD	0.8020 ± 0.073
PCDH-CMV-EF1-copGFP-Sirt1	0.978±0.056*
SRT1720	0.9953 ± 0.058*
EX527	0.5347 ± 0.069**

***P<0.05, ****P<0.01**

Title of the article: Effects of Sirt1 on Proliferation, Migration and Apoptosis of Endothelial Progenitor Cells in Peripheral Blood of SD Rats with Chronic Obstructive Pulmonary Disease

First author: Dong-Mei Sun, The First Affiliated Hospital of Hainan Medical University

Suppl Table 5. Adhesion and migration detection of EPCs. (A450 nm)

	OD	Number of migratory EPCs
COPD	0.284 ± 0.015	27±2.6
SRT1720	0.344 ± 0.029**	41±2.3***
EX527	0.26 ± 00.037	17.5±2**

***P<0.05, ****P<0.01, *****P<0.001**

Title of the article: Effects of Sirt1 on Proliferation, Migration and Apoptosis of Endothelial Progenitor Cells in Peripheral Blood of SD Rats with Chronic Obstructive Pulmonary Disease

First author: Dong-Mei Sun, The First Affiliated Hospital of Hainan Medical University

Suppl Table 6. The proportion of cells in each cell cycle phase and proportion of apoptotic cells. (%, n=3, $\bar{x}$±s)

	G_0G_1	G_2M	S	Apoptosis
COPD	85.3±0.35	4.8±0.50	8.4±0.57	7.3±0.35
SRT1720	80.1±0.21**	6.4±0.57*	11.3±0.42*	4.4±0.42*
EX527	87.5±0.35*	5.2±0.14	6.4±0.50	12.1±0.50**

***P<0.05, ****P<0.01**